

Zero-energy Bound States in Nodal Topological Lattice

Soo-Yong Lee, Gyungchoon Go, and Jung Hoon Han*
Department of Physics, Sungkyunkwan University, Suwon 440-746, Korea

Nodal topological lattice is a form of magnetic crystal with topologically non-trivial spin texture, that further exhibits a periodic array of nodes with vanishing magnetization. Electronic structure for conduction electrons strongly Hund-coupled to such nodal topological lattice is examined. Our findings show that each node attracts localized zero-energy states, protected by various symmetries, which form narrow bands through hybridization in a mid-gap region. Each of the nodal bands carry Chern numbers under suitable perturbations, indicating their potential role in the topological Hall effect. Significant enhancement of the density of states near zero energy that can be detected in a tunneling experiment will provide a signature of the formation of nodal topological lattice.

PACS numbers: 75.10.Hk, 72.15.-v, 75.70.Kw, 03.65.Ge

Introduction: Skyrmion crystal phase has been identified in chiral magnets minimally characterized by the Heisenberg ferromagnetic exchange and Dzyaloshinskii-Moriya (DM) interactions [1–3]. Magnetic field plays a key role for these materials in inducing a transition from the spiral ground state to the triple spiral phase, equivalent to the triangular lattice of Skyrmions. Although this is the most widely discovered form of topological spin lattice in chiral magnets so far, theory suggests many other types of possible topological lattices [4–6]. In two dimensions, superposition of two orthogonally propagating spirals results in the meron-anti-meron (MM) lattice with nodes (points of vanishing magnetization) also forming a periodic array. In three dimensions, multiple spiral phases are equivalent to a lattice of hedgehogs and anti-hedgehogs (HH) realizing simple cubic, or other crystal symmetries [6, 7]. Magnetization nodes accompany all of the known three-dimensional topological lattices constructed so far and remain robust against application of magnetic field, while the two-dimensional nodes are lifted by it. A recent observation of the Hall effect in MnGe is believed to be a consequence of three-dimensional simple cubic structure of HH lattice formed in that material [8–10].

Dynamics of conducting electrons coupled through strong Hund’s rule exchange to the topological lattice of local moments displays a fascinating array of phenomena dubbed “emergent electrodynamics” [3]. Several of its stark predictions such as the topological Hall effect and the analogue of Faraday’s law of induction has been confirmed experimentally [11]. Despite its remarkable successes, theory of emergent electrodynamics suffers from a subtlety concerning the interaction of electron with spins at the nodal points. Existing theories [12–14] rely on the large Hund’s exchange to kinetic energy ratio to assume a perfect alignment of local and itinerant spin moments. Such assumption obviously fails when the effective Hund coupling, given by the combined value $J|\mathbf{S}_\mathbf{r}|$, J =exchange energy, $\mathbf{S}_\mathbf{r}$ =local magnetization, turns to zero at the node. How to get around the adiabatic assumption for the nodal regions has remained

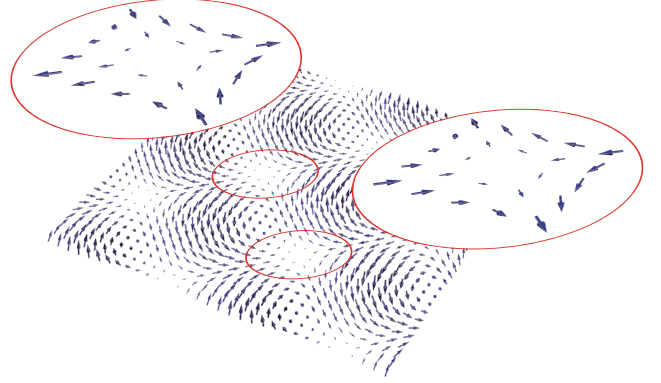


FIG. 1: (color online) Spin configuration of 2D MM lattice. There are two nodal points in the unit cell. Spin structure around each node is an anti-vortex as shown in insets.

unclear. In this paper we provide a fresh perspective on this issue by working out the electronic structure in interaction with the topological crystal phase with nodes, which we call the nodal topological lattice.

Zero-energy electronic states in nodal topological lattice: The interplay of conduction electrons through Hund’s coupling to the local moments is captured by a simple Hamiltonian

$$\begin{aligned}
 H &= H_K + H_J, \\
 H_K &= -t \sum_{\langle \mathbf{r}, \mathbf{r}' \rangle, \sigma = \uparrow, \downarrow} c_{\mathbf{r}, \sigma}^\dagger c_{\mathbf{r}', \sigma}, \\
 H_J &= -J \sum_{\mathbf{r}, \sigma, \sigma'} \mathbf{S}_\mathbf{r} \cdot (c_{\mathbf{r}, \sigma}^\dagger \boldsymbol{\sigma}_{\sigma, \sigma'} c_{\mathbf{r}, \sigma'}). \quad (1)
 \end{aligned}$$

To the zeroth order in t/J electronic energies occur at $\pm J|\mathbf{S}_\mathbf{r}|$, leaving a gap between $+J|\mathbf{S}_\mathbf{r}|_{min.}$ and $-J|\mathbf{S}_\mathbf{r}|_{min.}$. The adiabatic theory of emergent electrodynamics rests on a sufficiently large value of $J|\mathbf{S}_\mathbf{r}|_{min.}/t$ [12–14]. When there are nodes $|\mathbf{S}_\mathbf{r}|_{min.} = 0$ there will be two zero-energy states at $t = 0$, one for each spin orientation. As t increases, these nodal states

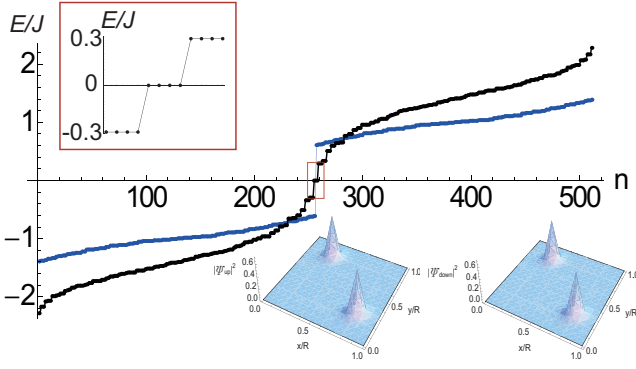


FIG. 2: (color online) Energies of the 2D \overline{MM} lattice for $t/J = 0.1$ and $R = 16$ (Black). There is no zero energy state in the case of a single spiral, $\mathbf{S} = (0, \cos Kx, \sin Kx)$ (Blue). Upper inset shows the enlarged plot of energies near $E = 0$. Lower plots are electronic densities of the four localized solutions with respect to up and down spin respectively.

remain exactly at, or sufficiently near, zero energy while all other states drift away to form bulk bands. Those localized states hybridize with each other to form narrow solitonic bands inside the bandgap region.

Existence of nodal zero-energy states for finite t/J can be confirmed by numerical diagonalization of the model Hamiltonian, first focusing on the 2D \overline{MM} lattice [5]

$$\mathbf{S}_{\mathbf{r}}^{\overline{MM}} = \left(\sin Ky, \cos Kx, \sin Kx + \cos Ky \right). \quad (2)$$

Coordinates $\mathbf{r} = (x, y)$ are integer-valued and $K = 2\pi/R$ for some integer choice of Skyrmion radius R . Nodes appear at $\mathbf{r}_1 = (1/4, 1/2)R$ and $\mathbf{r}_2 = (3/4, 0)R$ within the unit cell of size $R \times R$, both corresponding to local anti-vortex configurations as shown in Fig. 1. Separation between the nodes is half the unit cell: $\boldsymbol{\pi}_2 = (1/2, 1/2)R$. Choosing the lattice size equal to $R \times R$ and imposing periodic boundary condition, numerical solution of the model (1) containing one pair of meron and anti-meron structure is shown in Fig. 2. There are exactly four degenerate zero energy states inside a gap, each node attracting two localized solutions [15]. The four-fold degeneracy remains intact despite the proximity of the two nodal points. For larger lattices of size $mR \times nR$, $m, n \geq 1$, one finds $4 \times (m \times n)$ localized solutions out of which four remain strictly at zero energy.

For the 3D \overline{HH} lattice of simple cubic symmetry given by [5]

$$\mathbf{S}_{\mathbf{r}}^{\overline{HH}} = \mathbf{S}_{\mathbf{r}}^{\overline{MM}} + \left(\cos Kz, \sin Kz, 0 \right), \quad (3)$$

nodes appear at eight points in the unit cell of size R^3 . Hedgehogs are centered at $(1, 3, 5)R/8$, $(3, 5, 1)R/8$, $(5, 1, 3)R/8$, $(7, 7, 7)R/8$, while anti-hedgehog locations are displaced by $\boldsymbol{\pi}_3 = (1/2, 1/2, 1/2)R$ from each

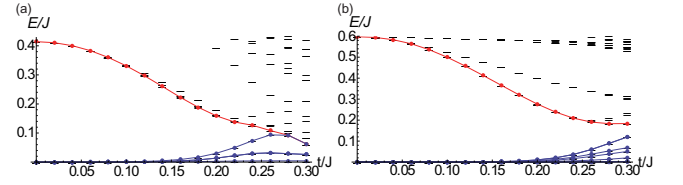


FIG. 3: (color online) Dependence of energy spectrum E/J on t/J in 3D (a) simple cubic (sc) and (b) face centered cubic (fcc) \overline{HH} lattices. Calculations are done for $R \times R \times R$ lattice, $R = 8$, and under periodic boundary condition. Bottom of the bulk energy band shown as red curves are clearly separated from the localized states for small t/J . There are 16 (32) almost degenerate localized states for sc (fcc) lattices.

hedgehog position. Electronic spectra show a total of 16 localized solutions per unit cell (two per node). Energies of the localized states are shown in Fig. 3.

Symmetries of nodal topological lattice: Applying the time-reversal operation $\Theta \equiv -i\sigma_y \mathcal{K}$ (\mathcal{K} =complex conjugation) on the Hamiltonian (1) gives

$$\Theta H_K = H_K \Theta, \quad \Theta H_J = -H_J \Theta. \quad (4)$$

The translation operator \mathcal{T} that moves each point by half the topological lattice spacing $\mathbf{r} \rightarrow \mathbf{r} + \boldsymbol{\pi}_d$ ($d = 2, 3$) has the property

$$\mathcal{T} H_K = H_K \mathcal{T}, \quad \mathcal{T} H_J = -H_J \mathcal{T}, \quad (5)$$

following from the fact that $\mathbf{S}_{\mathbf{r}+\boldsymbol{\pi}_d} = -\mathbf{S}_{\mathbf{r}}$ for the spin structure under consideration. Taking the product of the two mutually commuting operators to form a quasi-Kramers operator $\Lambda = \Theta \mathcal{T}$ ($\Lambda^2 = -\mathcal{T}^2$), one obtains $[H, \Lambda] = 0$. Further, on a R^d lattice with periodic boundary condition we also have $\mathcal{T}^2 = 1$, $\Lambda^2 = -1$, thus $|n\rangle$ and $\Lambda|n\rangle$ are indeed Kramers pairs. Another symmetry operation \mathcal{S} , $c_{\mathbf{r},\sigma} \rightarrow (-1)^i c_{\mathbf{r},\sigma}$, has the property

$$\mathcal{S} H_K = -H_K \mathcal{S}, \quad \mathcal{S} H_J = H_J \mathcal{S}. \quad (6)$$

The composite operator $\Omega = \Theta \mathcal{S}$ ($\Omega^2 = -1$) anti-commutes with the Hamiltonian $\{H, \Omega\} = 0$ while commuting with Λ , and serves as the particle-hole conjugation operator relating $|n\rangle$ with $\Omega|n\rangle$ of opposite sign of energy. Should a zero energy state $|\zeta\rangle$ exist, it must do so in quartet, $(|\zeta\rangle, \Lambda|\zeta\rangle, \Omega|\zeta\rangle, \Lambda\Omega|\zeta\rangle)$, in agreement with the numerical findings for two-dimensional \overline{MM} lattice.

Construction of zero-energy states: Zero-energy solutions around a single node can be constructed for $t/J \ll 1$. With the nodal position at the origin, the state has the expansion

$$|\zeta_1\rangle = |\mathbf{0}, \mathbf{S}_0\rangle + \sum_{\mathbf{r}} \left(-\frac{t}{J}\right)^{N_{\mathbf{r}}} [c_{\mathbf{r}}^+ |\mathbf{r}, \mathbf{S}_{\mathbf{r}}\rangle + c_{\mathbf{r}}^- |\mathbf{r}, -\mathbf{S}_{\mathbf{r}}\rangle] \quad (7)$$

in terms of the coherent states $|\mathbf{r}, \pm \mathbf{S}_{\mathbf{r}}\rangle$ of spin orientations $\pm \mathbf{S}_{\mathbf{r}}$ at the site \mathbf{r} . Absence of spin at the node allows certain freedom in choosing the nodal spin orientation \mathbf{S}_0 . $N_{\mathbf{r}}$ is the minimal number of steps in a path required to reach a given point \mathbf{r} starting from the node $\mathbf{0}$ (Recall that all such paths have the same $N_{\mathbf{r}}$). Schrödinger equation $H|\zeta_1\rangle = 0$ leads to the recursion relation for the amplitudes

$$c_{\mathbf{r}}^{\pm} = (\pm 1) \sum_{\delta} c_{\mathbf{r}-\delta}^{\pm} \frac{\langle \pm \mathbf{S}_{\mathbf{r}} | \pm \mathbf{S}_{\mathbf{r}-\delta} \rangle}{|\mathbf{S}_{\mathbf{r}}|}. \quad (8)$$

The sum involves the nearest neighbors of \mathbf{r} that lie closer to the origin than \mathbf{r} itself: $N_{\mathbf{r}-\delta} = N_{\mathbf{r}} - 1$. Ignoring $\langle -\mathbf{S}_{\mathbf{r}+\delta} | \mathbf{S}_{\mathbf{r}} \rangle$ as small compared to $\langle \mathbf{S}_{\mathbf{r}+\delta} | \mathbf{S}_{\mathbf{r}} \rangle$ for a smoothly varying spin background leads to the above simple recursion involving either $c_{\mathbf{r}}^+$'s or $c_{\mathbf{r}}^-$'s only. Extending the relation to the origin gives a discrete path sum,

$$c_{\mathbf{r}}^{\pm} = (\pm 1)^{N_{\mathbf{r}}} \sum_{\mathcal{C}} \frac{\langle \pm \mathbf{S}_{\mathbf{r}} | \pm \mathbf{S}_{\mathbf{r}'} \rangle}{|\mathbf{S}_{\mathbf{r}}|} \dots \frac{\langle \pm \mathbf{S}_1 | \mathbf{S}_0 \rangle}{|\mathbf{S}_1|}. \quad (9)$$

Each product inside the sum takes place along a particular path $\mathcal{C} = (\mathbf{0} \rightarrow \mathbf{r}_1 \rightarrow \dots \rightarrow \mathbf{r}' \rightarrow \mathbf{r})$ from the node to \mathbf{r} of length $N_{\mathbf{r}}$. Contributions of all equi-distant, distinct paths are summed over to give $c_{\mathbf{r}}^{\pm}$ above. A second zero-energy solution is found by $|\zeta_2\rangle = \Omega|\zeta_1\rangle$.

Zero-energy condition $H|\zeta_1\rangle = 0$ further requires

$$|\mathbf{S}_0\rangle = c_{\delta}^+ |\delta, \mathbf{S}_{\delta}\rangle - c_{\delta}^- |\delta, -\mathbf{S}_{\delta}\rangle$$

for each neighboring δ . To assign $|\mathbf{S}_0\rangle$ consistent with all of these requirements we must have [16]

$$\sum_{\delta} \mathbf{S}_{\delta} / |\mathbf{S}_{\delta}| = 0. \quad (10)$$

The sum of spin direction vectors surrounding the node has to be zero, as is fulfilled in both the 2D MM and 3D HH lattices under consideration.

Examining Eq. (9) in light of the identity $(\langle \mathbf{S}_{\mathbf{r}'} | \mathbf{S}_{\mathbf{r}} \rangle)^* = \langle -\mathbf{S}_{\mathbf{r}} | -\mathbf{S}_{\mathbf{r}'} \rangle$, we conclude that $|c_{\mathbf{r}}^+| = |c_{\mathbf{r}}^-|$ at all points \mathbf{r} provided $\langle \mathbf{S}_{\delta} | \mathbf{S}_0 \rangle$ is chosen to have the same amplitude as $\langle -\mathbf{S}_{\delta} | \mathbf{S}_0 \rangle$ for all the immediate neighbors δ of the origin. While this is not a necessary condition to guarantee a zero-energy state, such choice of \mathbf{S}_0 , if possible, ensures $|c_{\mathbf{r}}^+| = |c_{\mathbf{r}}^-|$ for all \mathbf{r} . The resulting zero-energy solution $|\zeta_1\rangle$ (as well as $|\zeta_2\rangle$) then would have the property that

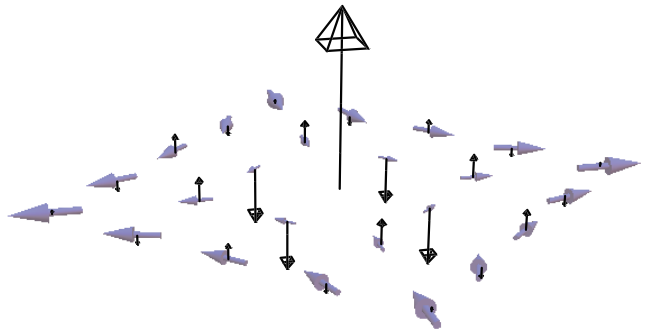


FIG. 4: Illustration of the zero energy state obtained from Eq. (7) when $\mathbf{S}_{\mathbf{r}} = K(y, x, 0)$ (grey arrows) and $t/J = 0.1$. Local average spin of zero energy state (solid arrows), $\langle \zeta_1 | \sigma_{\mathbf{r}} | \zeta_1 \rangle$, is perpendicular to $\mathbf{S}_{\mathbf{r}}$ when we choose $|c_{\mathbf{r}}^+| = |c_{\mathbf{r}}^-|$.

its spin average remains strictly orthogonal to the local magnetization: $\mathbf{S}_{\mathbf{r}} \cdot \langle \zeta_1 | \sigma_{\mathbf{r}} | \zeta_1 \rangle = 0 = \mathbf{S}_{\mathbf{r}} \cdot \langle \zeta_2 | \sigma_{\mathbf{r}} | \zeta_2 \rangle$. The zero-energy state, unable to favor either parallel or anti-parallel spin orientation, chooses to develop the polarization in the plane perpendicular to the local moment. In two dimension such choice of \mathbf{S}_0 is possible provided the four neighboring spins all lie in the plane, leaving an orthogonal direction for \mathbf{S}_0 . An explicit illustration of the zero-energy solution around the anti-vortex spin configuration, based on Eq. (9), is shown in Fig. 4. In 3D HH lattice choosing such \mathbf{S}_0 is generally impossible although zero-energy states can be constructed quite easily with Eqs. (9) and (10).

Taking Eq. (7) and Eq. (9) together it follows that the amplitude for $|\mathbf{r}, \mathbf{S}_{\mathbf{r}}\rangle$ fluctuates in sign between the two sub-lattices of the bi-partite lattice while the sign for $|\mathbf{r}, -\mathbf{S}_{\mathbf{r}}\rangle$ is smooth. Appropriate field theory model for zero-energy states can be constructed from the lattice Hamiltonian (1) after the unitary rotation $\Psi_{\mathbf{r}} = (c_{\mathbf{r},\uparrow} \ c_{\mathbf{r},\downarrow})^T = U_{\mathbf{r}}((-1)^{N_{\mathbf{r}}} c_{\mathbf{r},1} \ c_{\mathbf{r},2})^T$, $U_{\mathbf{r}}^\dagger (\mathbf{S}_{\mathbf{r}} \cdot \boldsymbol{\sigma}) U_{\mathbf{r}} = |\mathbf{S}_{\mathbf{r}}| \sigma^z$. The continuum theory as well as its localized solutions are discussed in SI.

Band structure of nodal lattice: Full electronic structure coupled to the nodal lattice is worked out in Figs. 5 and 6, for two and three dimensions, respectively. Nodal bands (induced by the periodic nodes in the magnetization) around $E = 0$ are indicated as red curves. At the Γ point, there are four degenerated states caused by the Λ and Ω symmetry. Note that $\Lambda^2 = -e^{ik \cdot 2\pi a}$ for a specific Bloch momentum \mathbf{k} . Quasi-Kramers degeneracy is guaranteed at the Γ and the M point (corner of the Brillouin zone) due to $\Lambda^2 = -1$.

Chern numbers in 2D appear for the central bands upon breaking of symmetries [17]. The quasi-time-reversal symmetry Λ is broken, for instance, by the Zeeman field $H_Z = -m_z \sum_{\mathbf{r}} (\hat{c}_{\mathbf{r},\uparrow}^\dagger \hat{c}_{\mathbf{r},\uparrow} - \hat{c}_{\mathbf{r},\downarrow}^\dagger \hat{c}_{\mathbf{r},\downarrow})$. Two outermost bands separate away from the two inner ones and take on Chern numbers ± 1 as shown in Fig. 5(b). The Ω

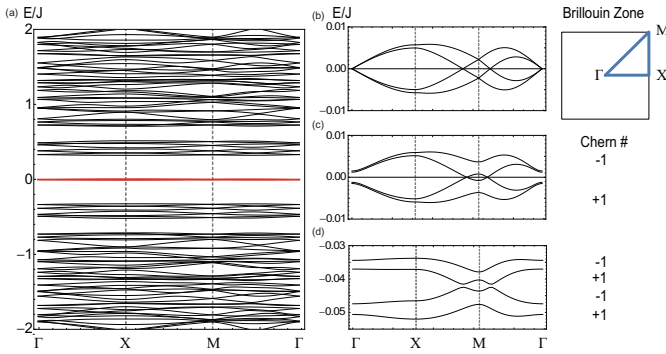


FIG. 5: (color online) (a) Electronic band structure for 2D MM lattice, using $t/J = 0.3$ and $R = 8$. Nodal bands are indicated as almost overlapping red lines. (b) Enlarged nodal bands at the zero magnetic field. (c) Magnetic field $m_z = 0.05J$ is added. Outer two bands are split away and carry Chern numbers. (d) NNN hopping $t' = 0.1t$ is added. All four nodal bands become non-degenerate and carry distinct Chern numbers indicated on right.

symmetry is broken by the next nearest neighbor (NNN) hopping, $H_{\text{NNN}} = -t' \sum_{\langle\langle \mathbf{r}, \mathbf{r}' \rangle\rangle} (\hat{c}_{\mathbf{r}, \uparrow}^\dagger \hat{c}_{\mathbf{r}', \uparrow} + \hat{c}_{\mathbf{r}, \downarrow}^\dagger \hat{c}_{\mathbf{r}', \downarrow})$. Now all the zero-energy bands have the Chern numbers shown in Fig. 5(c).

The 3D simple cubic HH band structure includes the 16 zero energy bands shown in Fig. 6. In the M point, the bands are degenerated as the Kramers pair. Due to the complexity of the calculation we have not attempted the calculation of the cross-sectional Chern numbers after all the band degeneracies are split. A reasonable expectation is that both the zero-energy bands and the bulk bands carry Chern numbers for a general cross section. A better and more direct manifestation of the zero-energy states may be the enhanced density of states (DOS) around $E = 0$, shown in Fig. 6(c).

Discussion: Several recent electronic structure calculations of MnGe reveal an extremely complex band pattern of this material [18–20]. A rough consensus among the theory suggests a Hund coupling $J_{\text{MnGe}} \simeq 2\text{eV}$, much bigger than the typical bandwidth of an individual band $t \simeq$ a few 100 meV found in the calculations [18–20]. The large J/t assumption used throughout this work is reasonably well justified for the majority-minority band pair in MnGe, suggesting that the formation of solitonic narrow bands half way between them is likely to accompany the HH formation. Extra states induced by the nodal lattice can be picked up by the DOS studies employing surface-sensitive STM or tunneling techniques. Zero modes protected by several lattice symmetries in our model investigation might spur a closer field-theoretical examination of models of zero-energy bound states.

This work is supported by the NRF grant (No.

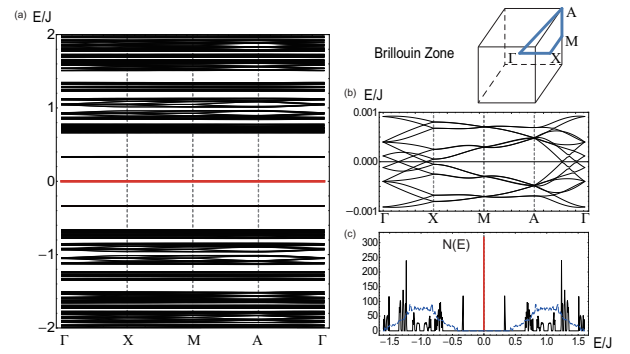


FIG. 6: (color online) (a) Electronic band structure for 3D simple cubic HH lattice using $t/J = 0.1$ and $R = 8$. Nodal bands are indicated as almost overlapping red lines. (b) Enlarged view of 16 nodal bands near zero energy. (c) Electronic DOS for HH lattice (black solid line, arbitrary units). A peak due to zero energy bands is clearly shown in solid red. Zero-energy DOS disappears when the magnetic texture is a simple spiral $\mathbf{S} = (0, \cos Kx, \sin Kx)$ (dashed blue curve).

2013R1A2A1A01006430). We acknowledge helpful discussions with Naoya Kanazawa, Bongjae Kim, Pajin Kim, Junhyun Lee, and Naoto Nagaosa for helpful discussions. J. H. H. would like to thank members of the MIT condensed matter theory group for their hospitality during his sabbatical leave.

* Electronic address: hanjh@skku.edu

- [1] S. Mühlbauer, B. Binz, F. Jonietz, C. Pfleiderer, A. Rosch, A. Neubauer, R. Georgii, and P. Böni, *Science* **323**, 915 (2009).
- [2] X. Z. Yu, Y. Onose, N. Kanazawa, J. H. Park, J. H. Han, Y. Matsui, N. Nagaosa, and Y. Tokura, *Nature (London)* **465**, 901 (2010).
- [3] Naoto Nagaosa and Yoshinori Tokura, *Nature Nanotechnology* **8**, 899 (2013).
- [4] U. K. Röfler, A. N. Bogdanov and C. Pfleiderer, *Nature (London)* **442**, 797 (2006).
- [5] Su Do Yi, Shigeki Onoda, Naoto Nagaosa, and Jung Hoon Han, *Phys. Rev. B* **80** 054416, (2009).
- [6] B. Binz, A. Vishwanath, and V. Aji, *Phys. Rev. Lett.* **96**, 207202 (2006); B. Binz and A. Vishwanath, *Phys. Rev. B* **74**, 214408 (2006).
- [7] Jin-Hong Park and Jung Hoon Han, *Phys. Rev. B* **83**, 184406 (2011).
- [8] N. Kanazawa, Y. Onose, T. Arima, D. Okuyama, K. Ohoyama, S. Wakimoto, K. Kakurai, S. Ishiwata, and Y. Tokura, *Phys. Rev. Lett.* **106**, 156603 (2011).
- [9] N. Kanazawa, J.-H. Kim, D. S. Inosov, J. S. White, N. Egetenmeyer, J. L. Gavilano, S. Ishiwata, Y. Onose, T. Arima, B. Keimer, and Y. Tokura, *Phys. Rev. B* **86** 134425, (2012).
- [10] O. L. Makarova, A. V. Tsvyashchenko, G. Andre, F. Porcher, L. N. Fomicheva, N. Rey, and I. Mirebeau, *Phys. Rev. B* **85**, 205205 (2012).
- [11] T. Schulz, R. Ritz, A. Bauer, M. Halder, M. Wagner,

- C. Franz, C. Pfleiderer, K. Everschor, M. Garst and A. Rosch, *Nature Physics* **8**, 301 (2012).
- [12] J. Ye, Y. B. Kim, A. J. Millis, B. I. Shraiman, P. Majumdar, and Z. Tesanovic, *Phys. Rev. Lett.* **83**, 3737 (1999).
- [13] B. Binz and A. Vishwanath, *Physica B* **403**, 1336 (2008).
- [14] Jiadong Zang, Maxim Mostovoy, Jung Hoon Han, and Naoto Nagaosa, *Phys. Rev. Lett.* **107** 136804 (2011).
- [15] Localized nature of the eigenstate can be checked through calculation of the state's inverse participation ratio, for example. Inclusion of higher harmonics in the magnetization profile produces the same number of nodal states at zero energy. The existence of node-localized states appear to be independent of the exact profile of the magnetization, only requiring the presence of nodes in it.
- [16] Supplementary information.
- [17] Haruki Watanabe, S. A. Parameswaran, S. Raghu, and Ashvin Vishwanath, *Phys. Rev. B* **90**, 045145 (2014).
- [18] U. K. Röbner, *J. Phys.: Conf. Ser.* **391**, 012104 (2012).
- [19] Mitchell I. Brickson and Dana A. Browne, *LA-SIGMA*, "Electronic and Magnetic Properties of MnGe" (2013).
- [20] M. Deutsch, O. L. Makarova, T. C. Hansen, M. T. Fernandez-Diaz, V. A. Sidorov, A. V. Tsvyashchenko, L. N. Fomicheva, F. Porcher, S. Petit, K. Koepnik, U. K. Röbner, and I. Mirebeau, *Phys. Rev. B* **89**, 180407(R) (2014).

Zero-energy Bound States in Nodal Topological Lattice: Supplementary Information

Soo-Yong Lee,¹ Gyungchoon Go,¹ and Jung Hoon Han^{1,2,*}

¹*Department of Physics, Sungkyunkwan University, Suwon 440-746, Korea*

²*Asia Pacific Center for Theoretical Physics, POSTECH, Pohang, Gyeongbuk 790-784, Korea*

I. ZERO ENERGY BOUND STATE IN THE ANTI-VORTEX

A. Lattice Model

We investigate the zero energy bound state under the generalized magnetization $\mathbf{S}_\mathbf{r}$ by performing the equation of motion. A trial zero energy state keeping up to leading order $(-\frac{t}{J})^{|\mathbf{N}_\mathbf{r}|}$ at each site \mathbf{r} is expressed by

$$|\zeta\rangle = |0, \mathbf{S}_0\rangle + \sum_{i \neq 0} \left(-\frac{t}{J}\right)^{|\mathbf{N}_\mathbf{r}|} [c_\mathbf{r}^+ |\mathbf{r}, \mathbf{S}_\mathbf{r}\rangle + c_\mathbf{r}^- |\mathbf{r}, -\mathbf{S}_\mathbf{r}\rangle], \quad (1.1)$$

where the magnetization $\mathbf{S}_\mathbf{r} = |\mathbf{S}_\mathbf{r}| (\cos \phi_\mathbf{r} \sin \theta_\mathbf{r}, \sin \phi_\mathbf{r} \sin \theta_\mathbf{r}, \cos \theta_\mathbf{r})$. Each local electronic state is spanned by the spin coherent states $|\mathbf{S}_\mathbf{r}\rangle = (\cos \frac{\theta_\mathbf{r}}{2}, e^{i\phi_\mathbf{r}} \sin \frac{\theta_\mathbf{r}}{2})^T$ and $|\mathbf{-S}_\mathbf{r}\rangle = (-e^{-i\phi_\mathbf{r}} \sin \frac{\theta_\mathbf{r}}{2}, \cos \frac{\theta_\mathbf{r}}{2})^T$, and the magnetization at the nodal point vanishes. We apply the trial zero energy state to the equation of motion, $H|\zeta\rangle = 0$. Each term gives

$$\begin{aligned} H_K |\zeta\rangle &= -t \sum_{\mathbf{r}, \mathbf{e}_\alpha} \left[\left(-\frac{t}{J}\right)^{|\mathbf{N}_\mathbf{r}-1|} [c_{\mathbf{r}-\mathbf{e}_\alpha}^+ \langle \mathbf{S}_\mathbf{r} | \mathbf{S}_{\mathbf{r}-\mathbf{e}_\alpha} \rangle |\mathbf{r}, \mathbf{S}_\mathbf{r}\rangle + c_{\mathbf{r}-\mathbf{e}_\alpha}^- \langle -\mathbf{S}_\mathbf{r} | \mathbf{S}_{\mathbf{r}-\mathbf{e}_\alpha} \rangle |\mathbf{r}, -\mathbf{S}_\mathbf{r}\rangle] \right. \\ &+ \left(-\frac{t}{J}\right)^{|\mathbf{N}_\mathbf{r}-1|} [c_{\mathbf{r}-\mathbf{e}_\alpha}^- \langle \mathbf{S}_\mathbf{r} | -\mathbf{S}_{\mathbf{r}-\mathbf{e}_\alpha} \rangle |\mathbf{r}, \mathbf{S}_\mathbf{r}\rangle + c_{\mathbf{r}-\mathbf{e}_\alpha}^+ \langle -\mathbf{S}_\mathbf{r} | -\mathbf{S}_{\mathbf{r}-\mathbf{e}_\alpha} \rangle |\mathbf{r}, -\mathbf{S}_\mathbf{r}\rangle] \\ &+ \left(-\frac{t}{J}\right)^{|\mathbf{N}_\mathbf{r}+1|} [c_{\mathbf{r}+\mathbf{e}_\alpha}^+ \langle \mathbf{S}_\mathbf{r} | \mathbf{S}_{\mathbf{r}+\mathbf{e}_\alpha} \rangle |\mathbf{r}, \mathbf{S}_\mathbf{r}\rangle + c_{\mathbf{r}+\mathbf{e}_\alpha}^- \langle -\mathbf{S}_\mathbf{r} | \mathbf{S}_{\mathbf{r}+\mathbf{e}_\alpha} \rangle |\mathbf{r}, -\mathbf{S}_\mathbf{r}\rangle] \\ &+ \left(-\frac{t}{J}\right)^{|\mathbf{N}_\mathbf{r}+1|} [c_{\mathbf{r}+\mathbf{e}_\alpha}^- \langle \mathbf{S}_\mathbf{r} | -\mathbf{S}_{\mathbf{r}+\mathbf{e}_\alpha} \rangle |\mathbf{r}, \mathbf{S}_\mathbf{r}\rangle + c_{\mathbf{r}+\mathbf{e}_\alpha}^+ \langle -\mathbf{S}_\mathbf{r} | -\mathbf{S}_{\mathbf{r}+\mathbf{e}_\alpha} \rangle |\mathbf{r}, -\mathbf{S}_\mathbf{r}\rangle] \\ &\simeq -t \sum_{\mathbf{r}, \mathbf{e}_\alpha} \left[\left(-\frac{t}{J}\right)^{|\mathbf{N}_\mathbf{r}-1|} [c_{\mathbf{r}-\mathbf{e}_\alpha}^+ \langle \mathbf{S}_\mathbf{r} | \mathbf{S}_{\mathbf{r}-\mathbf{e}_\alpha} \rangle |\mathbf{r}, \mathbf{S}_\mathbf{r}\rangle + \left(-\frac{t}{J}\right)^{|\mathbf{N}_\mathbf{r}-1|} [c_{\mathbf{r}-1}^- \langle -\mathbf{S}_\mathbf{r} | -\mathbf{S}_{\mathbf{r}-\mathbf{e}_\alpha} \rangle |\mathbf{r}, -\mathbf{S}_\mathbf{r}\rangle] \right. \\ &+ \left(-\frac{t}{J}\right)^{|\mathbf{N}_\mathbf{r}+1|} [c_{\mathbf{r}+\mathbf{e}_\alpha}^+ \langle \mathbf{S}_\mathbf{r} | \mathbf{S}_{\mathbf{r}+\mathbf{e}_\alpha} \rangle |\mathbf{r}, \mathbf{S}_\mathbf{r}\rangle] + \left(-\frac{t}{J}\right)^{|\mathbf{N}_\mathbf{r}+1|} [c_{\mathbf{r}+\mathbf{e}_\alpha}^- \langle -\mathbf{S}_\mathbf{r} | -\mathbf{S}_{\mathbf{r}+\mathbf{e}_\alpha} \rangle |\mathbf{r}, -\mathbf{S}_\mathbf{r}\rangle] \end{aligned} \quad (1.2)$$

and

$$H_J |\zeta\rangle = -J \sum_{\mathbf{r} \neq 0} \left(-\frac{t}{J}\right)^{|\mathbf{N}_\mathbf{r}|} |\mathbf{S}_\mathbf{r}| [c_\mathbf{r}^+ |\mathbf{r}, \mathbf{S}_\mathbf{r}\rangle - c_\mathbf{r}^- |\mathbf{r}, -\mathbf{S}_\mathbf{r}\rangle]. \quad (1.3)$$

We assume that the spin is adiabatically changed, $\langle \mathbf{S}_\mathbf{r} | -\mathbf{S}_{\mathbf{r}+\mathbf{e}_\alpha} \rangle = 0$, when following the smooth magnetization except the node. To cancel above two terms each other, one satisfies

$$\begin{aligned} c_{\mathbf{r}-\mathbf{e}_\alpha}^+ \langle \mathbf{S}_\mathbf{r} | \mathbf{S}_{\mathbf{r}-\mathbf{e}_\alpha} \rangle + \left(-\frac{t}{J}\right)^2 c_{\mathbf{r}+\mathbf{e}_\alpha}^+ \langle \mathbf{S}_\mathbf{r} | \mathbf{S}_{\mathbf{r}+\mathbf{e}_\alpha} \rangle - c_\mathbf{r}^+ |\mathbf{S}_\mathbf{r}| &= 0, \\ c_{\mathbf{r}-\mathbf{e}_\alpha}^- \langle -\mathbf{S}_\mathbf{r} | -\mathbf{S}_{\mathbf{r}-\mathbf{e}_\alpha} \rangle + \left(-\frac{t}{J}\right)^2 c_{\mathbf{r}+\mathbf{e}_\alpha}^- \langle -\mathbf{S}_\mathbf{r} | -\mathbf{S}_{\mathbf{r}+\mathbf{e}_\alpha} \rangle + c_\mathbf{r}^- |\mathbf{S}_\mathbf{r}| &= 0 \end{aligned} \quad (1.4)$$

for $N_\mathbf{r} > 1$. In the small $\frac{t}{J}$ limit, the spin overlap under the smoothly varying circumstance is $\langle \mathbf{S}_\mathbf{r} | \mathbf{S}_{\mathbf{r} \pm \mathbf{e}_\alpha} \rangle \sim \mathcal{O}(1) \gg \frac{t}{J}$. Thus, we neglect the second term of Eq. (1.4) and simplify $c_\mathbf{r}^+$ and $c_\mathbf{r}^-$ as

$$\begin{aligned} c_\mathbf{r}^+ &\simeq \sum_{\mathbf{e}_\alpha} c_{\mathbf{r}-\mathbf{e}_\alpha}^+ \frac{\langle \mathbf{S}_\mathbf{r} | \mathbf{S}_{\mathbf{r}-\mathbf{e}_\alpha} \rangle}{|\mathbf{S}_\mathbf{r}|} = \sum_{\mathbf{c}} \frac{\langle \pm \mathbf{S}_\mathbf{r} | \pm \mathbf{S}_{\mathbf{r}'} \rangle}{|\mathbf{S}_\mathbf{r}|} \dots \frac{\langle \pm \mathbf{S}_2 | \mathbf{S}_1 \rangle}{|\mathbf{S}_2|} c_1^+ \\ c_\mathbf{r}^- &\simeq \sum_{\mathbf{e}_\alpha} -c_{\mathbf{r}-\mathbf{e}_\alpha}^- \frac{\langle -\mathbf{S}_\mathbf{r} | -\mathbf{S}_{\mathbf{r}-\mathbf{e}_\alpha} \rangle}{|\mathbf{S}_\mathbf{r}|} = (-1)^{N_\mathbf{r}-1} \sum_{\mathbf{c}} \frac{\langle \pm \mathbf{S}_\mathbf{r} | \pm \mathbf{S}_{\mathbf{r}'} \rangle}{|\mathbf{S}_\mathbf{r}|} \dots \frac{\langle \pm \mathbf{S}_2 | \mathbf{S}_1 \rangle}{|\mathbf{S}_2|} c_1^-. \end{aligned} \quad (1.5)$$

\mathbf{S}_N is a spin vector located in hopping distance $N_{\mathbf{r}}$. \mathcal{C} stands for a particular path ($\mathbf{r}_1 \rightarrow \dots \rightarrow \mathbf{r}' \rightarrow \mathbf{r}$) from the nearest vicinity of the node to \mathbf{r} . To make a connection between the node and its vicinity $\boldsymbol{\delta} = \mathbf{r}_1$, the coefficients keeping up to the leading order are determined by the equation of motion,

$$-|\mathbf{S}_0\rangle + |\mathbf{S}_\delta|[c_\delta^+|\mathbf{S}_\delta\rangle - c_\delta^-|-\mathbf{S}_\delta\rangle] = 0. \quad (1.6)$$

If the node state is $|\mathbf{S}_0\rangle = (\alpha, \beta)^T$, the coefficients are

$$c_\delta^+ = \frac{1}{|\mathbf{S}_\delta|} \left(\alpha \cos \frac{\theta_\delta}{2} + \beta e^{-i\phi_\delta} \sin \frac{\theta_\delta}{2} \right) = \frac{1}{|\mathbf{S}_\delta|} \langle \mathbf{S}_\delta | \mathbf{S}_0 \rangle \quad c_\delta^- = \frac{1}{|\mathbf{S}_\delta|} \left(\alpha e^{i\phi_\delta} \sin \frac{\theta_\delta}{2} - \beta \cos \frac{\theta_\delta}{2} \right) = -\frac{1}{|\mathbf{S}_\delta|} \langle -\mathbf{S}_\delta | \mathbf{S}_0 \rangle. \quad (1.7)$$

Inserting c_δ^\pm into the equation of motion at $\mathbf{r} = 0$,

$$\sum_{\boldsymbol{\delta}} c_\delta^+ |\mathbf{S}_\delta\rangle + c_\delta^- |-\mathbf{S}_\delta\rangle = 0,$$

we thus obtain

$$\sum_{\boldsymbol{\delta}} \mathbf{S}_\delta / |\mathbf{S}_\delta| = 0. \quad (1.8)$$

This result shows that the zero energy state always appears when the sum of the spin direction vectors of the vicinity vanishes in the large J limit. We also note that the spin vector of the zero energy state at each \mathbf{r} , $\langle \zeta | \boldsymbol{\sigma}_{\mathbf{r}} | \zeta \rangle$, always becomes perpendicular to $\mathbf{S}_{\mathbf{r}}$ when $|c_\delta^+|^2 = |c_\delta^-|^2$ for all $\boldsymbol{\delta}$ because $\mathbf{S}_{\mathbf{r}} \cdot \boldsymbol{\sigma}_{\mathbf{r}} | \pm \mathbf{S}_{\mathbf{r}} \rangle = \pm |\mathbf{S}_{\mathbf{r}}| | \pm \mathbf{S}_{\mathbf{r}} \rangle$ by the definition of the spin coherent state.

B. Continuum Limit

In this section, we investigate the zero energy bound state around the anti-vortex in 2D by performing the equation of motion in the continuum limit. We consider that, in the vicinity of the node, the magnetic texture is composed of the anti-vortex,

$$\mathbf{S}(\mathbf{r}) = S(r)(y, x, 0), \quad (1.9)$$

where $r^2 = x^2 + y^2$, $x = r \cos \theta$ and $y = r \sin \theta$. Spin coherent states of the local magnetic moment at \mathbf{r} are $|\mathbf{S}_{\mathbf{r}}\rangle = \frac{1}{\sqrt{2}} \begin{pmatrix} 1 \\ ie^{-i\theta} \end{pmatrix}$ along the the spin parallel direction, and are $|-\mathbf{S}_{\mathbf{r}}\rangle = |\bar{\mathbf{S}}_{\mathbf{r}}\rangle = \frac{1}{\sqrt{2}} \begin{pmatrix} ie^{i\theta} \\ 1 \end{pmatrix}$ along the the spin anti-parallel direction. The electron operator basis along the spin parallel or antiparallel can be changed by an unitary transformation, $\hat{c}_{\mathbf{r}} = U(\mathbf{r})\hat{a}_{\mathbf{r}}$, where $U(\mathbf{r}) = \frac{1}{\sqrt{2}} \begin{pmatrix} 1 & -ie^{i\theta} \\ -ie^{-i\theta} & 1 \end{pmatrix}$ with $\hat{c}_{\mathbf{r}} = \begin{pmatrix} \hat{c}_{\uparrow, \mathbf{r}} \\ \hat{c}_{\downarrow, \mathbf{r}} \end{pmatrix}$ and $\hat{a}_{\mathbf{r}} = \begin{pmatrix} \hat{a}_{\mathbf{S}, \mathbf{r}} \\ \hat{a}_{\bar{\mathbf{S}}, \mathbf{r}} \end{pmatrix}$. We begin with the transformed kinetic Hamiltonian,

$$\begin{aligned} H_K &= -t \sum_{\mathbf{r}, \boldsymbol{\delta} = \{\pm a\hat{x}, \pm a\hat{y}\}} \hat{c}_{A, \mathbf{r}}^\dagger \hat{c}_{B, \mathbf{r} + \boldsymbol{\delta}} + h.c. \\ &= -t \sum_{\mathbf{r}, \boldsymbol{\delta} = \{\pm a\hat{x}, \pm a\hat{y}\}} \hat{a}_{A, \mathbf{r}}^\dagger U^\dagger(\mathbf{r}) U(\mathbf{r} + \boldsymbol{\delta}) \hat{a}_{B, \mathbf{r} + \boldsymbol{\delta}} + h.c. \\ &= -t \sum_{\mathbf{r}, \boldsymbol{\delta} = \{a\hat{x}, a\hat{y}\}} 2\hat{a}_{A, \mathbf{r}}^\dagger \hat{a}_{B, \mathbf{r}} + \hat{a}_{A, \mathbf{r}}^\dagger (\boldsymbol{\delta} \cdot \boldsymbol{\nabla})^2 \hat{a}_{B, \mathbf{r}} + \hat{a}_{A, \mathbf{r}}^\dagger U^\dagger(\mathbf{r}) [(\boldsymbol{\delta} \cdot \boldsymbol{\nabla})^2 U(\mathbf{r})] \hat{a}_{B, \mathbf{r}} \\ &\quad + 2\hat{a}_{A, \mathbf{r}}^\dagger U^\dagger(\mathbf{r}) [(\boldsymbol{\delta} \cdot \boldsymbol{\nabla}) U(\mathbf{r})] [(\boldsymbol{\delta} \cdot \boldsymbol{\nabla}) \hat{a}_{B, \mathbf{r}}] + h.c. + \mathcal{O}(\delta^3). \end{aligned} \quad (1.10)$$

where $U(\mathbf{r} + \boldsymbol{\delta}) = U(\mathbf{r}) + (\boldsymbol{\delta} \cdot \boldsymbol{\nabla}) U(\mathbf{r}) + \frac{1}{2} (\boldsymbol{\delta} \cdot \boldsymbol{\nabla})^2 U(\mathbf{r}) + \mathcal{O}(\delta^3)$ and $\hat{a}_{\mathbf{r} + \boldsymbol{\delta}} = \hat{a}_{\mathbf{r}} + (\boldsymbol{\delta} \cdot \boldsymbol{\nabla}) \hat{a}_{\mathbf{r}} + \frac{1}{2} (\boldsymbol{\delta} \cdot \boldsymbol{\nabla})^2 \hat{a}_{\mathbf{r}} + \mathcal{O}(\delta^3)$. We use some vector identities

$$\begin{aligned} \sum_{\boldsymbol{\delta} = \{a\hat{x}, a\hat{y}\}} U^\dagger(\mathbf{r}) (\boldsymbol{\delta} \cdot \boldsymbol{\nabla})^2 U(\mathbf{r}) &= \frac{1}{2r^2} \begin{pmatrix} -1 & ie^{i\theta} \\ ie^{-i\theta} & -1 \end{pmatrix}, \text{ and} \\ \sum_{\boldsymbol{\delta} = \{a\hat{x}, a\hat{y}\}} U^\dagger(\mathbf{r}) [(\boldsymbol{\delta} \cdot \boldsymbol{\nabla}) U(\mathbf{r})] (\boldsymbol{\delta} \cdot \boldsymbol{\nabla}) &= \frac{1}{2r^2} \begin{pmatrix} -i\partial_\theta & e^{i\theta} \partial_\theta \\ -e^{-i\theta} \partial_\theta & i\partial_\theta \end{pmatrix}. \end{aligned} \quad (1.11)$$

Thus the kinetic Hamiltonian is simplified

$$H_K = -t \sum_{\mathbf{r}} \hat{a}_{A,\mathbf{r}}^\dagger [4 + \nabla^2 + \frac{1}{r^2} \begin{pmatrix} -i\partial_\theta - \frac{1}{2} & e^{i\theta} [\frac{i}{2} + \partial_\theta] \\ e^{-i\theta} [\frac{i}{2} - \partial_\theta] & i\partial_\theta - \frac{1}{2} \end{pmatrix}] \hat{a}_{B,\mathbf{r}} + h.c. + \mathcal{O}(\delta^4). \quad (1.12)$$

Recalling the result of the lattice calculation in the main text, the sign of $|\mathbf{S}\rangle$ is changed depending on the sublattice A and B . We set $\hat{a}_{B,\mathbf{S}} \rightarrow -\hat{a}_{B,\mathbf{S}}$. In the adiabatic limit by large J except the node, the terms by the overlap between $|\mathbf{S}\rangle$ and $|\bar{\mathbf{S}}\rangle$ can be neglected as described above. Adding the Hund term $H_J = -J \sum_{\mathbf{r}} \hat{a}_{A,\mathbf{r}}^\dagger \tau_z \hat{a}_{A,\mathbf{r}} + \hat{a}_{B,\mathbf{r}}^\dagger \tau_z \hat{a}_{B,\mathbf{r}}$ with $\hat{a}_{i,\mathbf{r}} = \begin{pmatrix} \hat{a}_{i,\mathbf{S},\mathbf{r}} \\ \hat{a}_{i,\bar{\mathbf{S}},\mathbf{r}} \end{pmatrix}$ and $i \in \{A, B\}$, we obtain the total Hamiltonian

$$H = t\chi^\dagger \begin{pmatrix} -J'S(\mathbf{r}) & 4 + \nabla^2 + \frac{1}{r^2}[-i\partial_\theta - \frac{1}{2}] & 0 & 0 \\ 4 + \nabla^2 + \frac{1}{r^2}[i\partial_\theta - \frac{1}{2}] & -J'S(\mathbf{r}) & 0 & 0 \\ 0 & 0 & J'S(\mathbf{r}) & -4 - \nabla^2 - \frac{1}{r^2}[i\partial_\theta - \frac{1}{2}] \\ 0 & 0 & -4 - \nabla^2 - \frac{1}{r^2}[-i\partial_\theta - \frac{1}{2}] & J'S(\mathbf{r}) \end{pmatrix} \chi, \quad (1.13)$$

where $\chi^\dagger = \begin{pmatrix} \hat{a}_{\mathbf{S},A}^\dagger & -\hat{a}_{\mathbf{S},B}^\dagger & \hat{a}_{\bar{\mathbf{S}},A}^\dagger & \hat{a}_{\bar{\mathbf{S}},B}^\dagger \end{pmatrix}$ and $J' = J/t$. To find the zero energy state, one can separate the 2×2 block diagonal matrices, $H_+ \otimes H_-$. We choose the first block diagonal H_+ . Since $[H_\pm, -i\partial_\theta] = 0$, there is a good quantum number corresponding to the angular momentum. The zero energy wavefunctions are $u(\mathbf{r})e^{im\theta}$ for the spin-parallel state at the A sublattice, and are $-v(\mathbf{r})e^{in\theta}$ for the spin-parallel state at the B sublattice. The simultaneous differential equations are given by

$$\begin{aligned} -J'S(r)u(r)e^{im\theta} + [4 + \partial_r^2 + \frac{1}{r}\partial_r - \frac{1}{r^2}[n^2 - n + \frac{1}{2}]]v(r)e^{in\theta} &= 0, \text{ and} \\ -J'S(r)v(r)e^{in\theta} + [4 + \partial_r^2 + \frac{1}{r}\partial_r - \frac{1}{r^2}[m^2 + m + \frac{1}{2}]]u(r)e^{im\theta} &= 0. \end{aligned} \quad (1.14)$$

To satisfy the simultaneous equations, the angular dependence m and n should be same. For simplicity, we transform $u(r) = \frac{1}{\sqrt{r}}\alpha(r)$ and $v(r) = \frac{1}{\sqrt{r}}\beta(r)$. The modified equations are

$$\begin{aligned} -J'S(r)\alpha(r) + [4 + \partial_r^2 - \frac{(m - \frac{1}{2})^2}{r^2}]\beta(r) &= 0, \text{ and} \\ -J'S(r)\beta(r) + [4 + \partial_r^2 - \frac{(m + \frac{1}{2})^2}{r^2}]\alpha(r) &= 0. \end{aligned} \quad (1.15)$$

$\alpha(r)$ can be the same as $\beta(r)$ because of the continuity of A and B sublattice, which happens when a characteristic length scale by the low-energy kinetic momentum is much larger than the lattice constant, $1/\nabla \gg a$. Thus, $m = 0$ and the equation then simply becomes

$$\partial_r^2 \alpha(r) - Q(r)\alpha(r) = 0, \quad (1.16)$$

where $Q(r) = -4 + \frac{1}{4r^2} + J'S(r)$. Applying the WKB approximation to solve the second order linear differential equation for the zero energy solution, one finds

$$\alpha(r) = \beta(r) \sim \begin{cases} \frac{\exp[\pm \int^r dr' \sqrt{Q(r')}]}{|Q(r)|^{1/4}} & \text{for } Q(r') > 0 \\ \frac{\exp[\pm i \int^r dr' \sqrt{|Q(r')|}]}{|Q(r)|^{1/4}} & \text{for } Q(r') < 0 \end{cases}. \quad (1.17)$$

The extended ($Q(r) < 0$) and localized ($Q(r) > 0$) solutions near r_0 when $Q(r_0) = 0$ can be connected to be differentiable. If the $S(r)$ is a increasing function of r , the zero energy state starts being localized from the place where $Q(r) > 0$. Once the magnetization is saturated as $S(r) = S_0$ in $r \rightarrow \infty$, the localized zero energy solution always exists for the $J'S_0 > 4$ case as

$$u(r) = v(r) \sim \frac{1}{\sqrt{r}} e^{-\sqrt{J'S_0 - 4}r}. \quad (1.18)$$

At the node, this continuum theory is not applicable, but if Eq. (1.8) holds, the zero energy state is still guaranteed on the lattice.

II. BAND THEORY

The Fourier transformation of the Hamiltonian in the reciprocal space \mathbf{k} is reexpressed by $\mathbf{S}_{\mathbf{r}} = \sum_{\mathbf{K}} \mathbf{S}_{\mathbf{K}} e^{i\mathbf{K}\cdot\mathbf{r}}$ and $\hat{c}_{\mathbf{r}} = \frac{1}{L^{d/2}} \sum_{\mathbf{q}} e^{i\mathbf{q}\cdot\mathbf{r}} \hat{c}_{\mathbf{q}}$ as

$$\mathcal{H} = -2t \sum_{\mathbf{q}, \sigma} \left[\cos q_x a + \cos q_y a \right] \hat{c}_{\mathbf{q}, \sigma}^\dagger \hat{c}_{\mathbf{q}, \sigma} - J \sum_{\mathbf{K}', \sigma, \sigma'} \mathbf{S}_{\mathbf{K}'} \cdot \hat{c}_{\mathbf{q}, \sigma}^\dagger \boldsymbol{\sigma}_{\sigma, \sigma'} \hat{c}_{\mathbf{q}-\mathbf{K}', \sigma'} \quad (2.1)$$

After setting $\mathbf{q} \rightarrow \mathbf{k} - \mathbf{K}$, $\mathbf{K}' \rightarrow \mathbf{K}' - \mathbf{K}$ and then $\mathbf{K}, \mathbf{K}' \rightarrow -\mathbf{K}, -\mathbf{K}'$, the Hamiltonian at \mathbf{k} is

$$\mathcal{H}(\mathbf{k}) = -2t \sum_{\mathbf{K}, \sigma} \left[\cos(k_x + \mathbf{K})a + \cos(k_y + \mathbf{K})a \right] \hat{c}_{\mathbf{k}, \sigma}^\dagger \hat{c}_{\mathbf{k}, \sigma} - J_{\text{H}} \sum_{\mathbf{K}, \mathbf{K}', \sigma, \sigma'} \mathbf{S}_{\mathbf{K}-\mathbf{K}'} \cdot \hat{c}_{\mathbf{k}+\mathbf{K}, \sigma'}^\dagger \boldsymbol{\sigma}_{\sigma, \sigma'} \hat{c}_{\mathbf{k}+\mathbf{K}', \sigma'}. \quad (2.2)$$

After rewriting $\hat{c}_{\sigma, \mathbf{k}+\mathbf{K}} \rightarrow \hat{c}_{\sigma, \mathbf{K}}(\mathbf{k})$, one finds that

$$\mathcal{H}(\mathbf{k}) = \sum_{\mathbf{K}, \mathbf{K}'} \hat{c}_{\sigma, \mathbf{K}}^\dagger(\mathbf{k}) \mathcal{H}_{\sigma, \sigma', \mathbf{K}\mathbf{K}'}(\mathbf{k}) \hat{c}_{\sigma', \mathbf{K}'}(\mathbf{k}), \quad (2.3)$$

where

$$\mathcal{H}_{\sigma, \sigma', \mathbf{K}\mathbf{K}'}(\mathbf{k}) = -2t \left[\cos(k_x + \mathbf{K})a + \cos(k_y + \mathbf{K})a \right] \delta_{\mathbf{K}, \mathbf{K}'} \delta_{\sigma, \sigma'} - J \mathbf{S}_{\mathbf{K}-\mathbf{K}'} \cdot \boldsymbol{\sigma}_{\sigma, \sigma'}. \quad (2.4)$$

The Bloch wavefunction at the crystal momentum \mathbf{k} is $\psi_{\sigma, \mathbf{k}} = e^{i\mathbf{k}\cdot\mathbf{r}} \sum_{\mathbf{K}} \hat{c}_{\sigma, \mathbf{k}-\mathbf{K}} e^{-i\mathbf{K}\cdot\mathbf{r}}$. At the momentum space, the magnetic structure of the 2D $\overline{\text{MM}}$ in Eq. (2) of the main text can be reexpressed

$$\begin{aligned} \mathbf{S}_{2D, \mathbf{K}} &= \int d\mathbf{r} e^{-i\mathbf{K}\cdot\mathbf{r}} \mathbf{S}_{2D, \mathbf{r}} \\ &= \frac{1}{2} \left([-i\delta_{\mathbf{K}, K_y \hat{y}} + i\delta_{\mathbf{K}, -K_y \hat{y}}], [\delta_{\mathbf{K}, K_x \hat{x}} + \delta_{\mathbf{K}, -K_x \hat{x}}], [-i\delta_{\mathbf{K}, K_x \hat{x}} + i\delta_{\mathbf{K}, -K_x \hat{x}}] + [\delta_{\mathbf{K}, K_y \hat{y}} + \delta_{\mathbf{K}, -K_y \hat{y}}] \right). \end{aligned} \quad (2.5)$$

The 3D $\overline{\text{HH}}$ structure in Eq. (3) of the main text also can be reexpressed

$$\begin{aligned} \mathbf{S}_{3D, \mathbf{K}} &= \int d\mathbf{r} e^{-i\mathbf{K}\cdot\mathbf{r}} \mathbf{S}_{3D, \mathbf{r}} \\ &= \mathbf{S}_{2D, \mathbf{K}} + \frac{1}{2} \left([\delta_{\mathbf{K}, K_z \hat{z}} + \delta_{\mathbf{K}, -K_z \hat{z}}], [-i\delta_{\mathbf{K}, K_z \hat{z}} + i\delta_{\mathbf{K}, -K_z \hat{z}}], 0 \right). \end{aligned} \quad (2.6)$$

After diagonalizing Eq. (2.3) at each \mathbf{k} , we obtain the bandstructures of 2D $\overline{\text{MM}}$ and 3D $\overline{\text{HH}}$ topological lattices in the reduced Brillouin zone.

* Electronic address: hanjh@skku.edu